



華東理工大學

EAST CHINA UNIVERSITY OF SCIENCE AND TECHNOLOGY



CoSW: Conditional Sample Weighting for Smoke Segmentation with Label Noise

Lujian Yao, Haitao Zhao*, Zhongze Wang, Kaijie Zhao, Jingchao Peng

East China University of Science and Technology

Smoke Segmentation

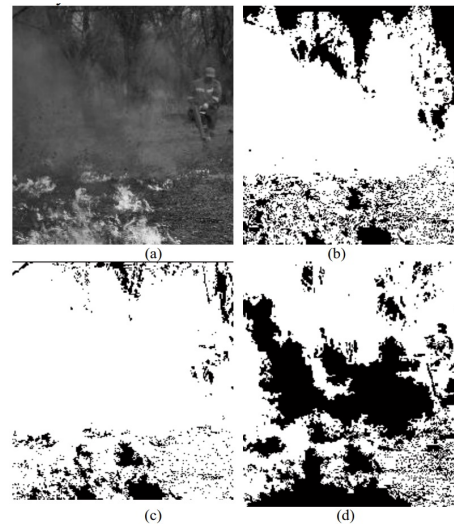
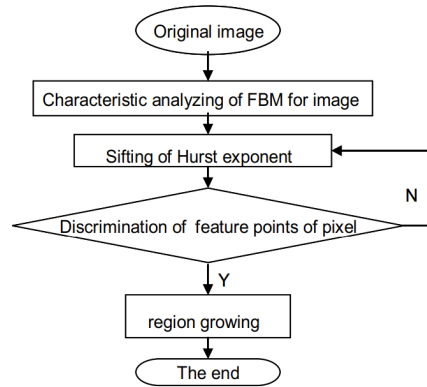
- In wildlife, smoke is an important indicator of **fire**. ESS enables **rapid** identification of the location of the **smoke source**, facilitating the timely extinguishing of the flames by rescue personnel and **preventing the occurrence of large fires**.
- In industrial production, ESS can also aid in promptly detecting the location of **gas leaks** and prevent **the spread of toxic and harmful gases**.



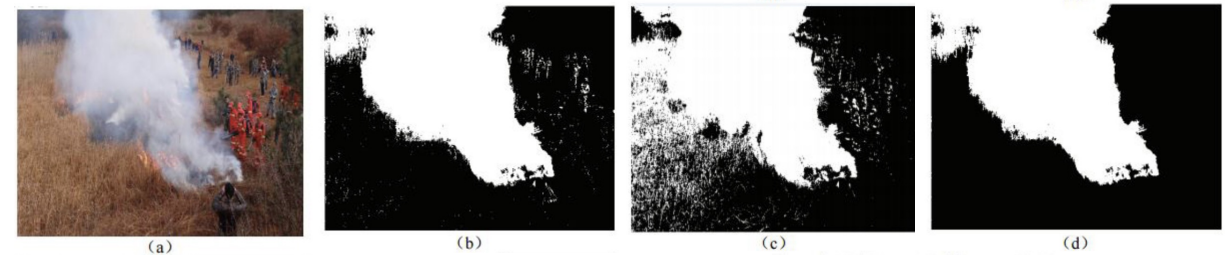
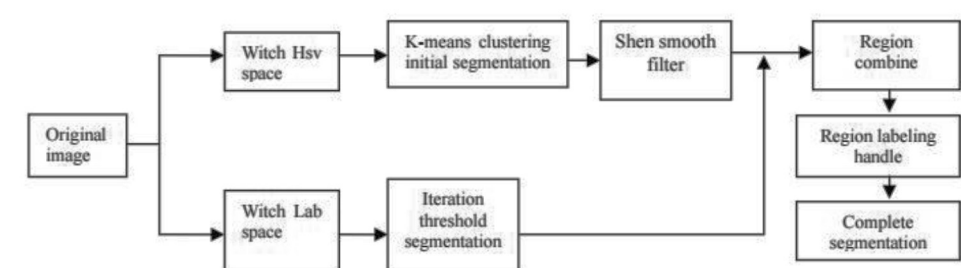
Traditional Smoke Segmentation

In smoke segmentation, **the color and texture features** of smoke play a significant role. **color enhancement** techniques and **color channel analysis** to segment smoke regions

Region Growing [1]



Color Space [2]



[1] Wang X, Jiang A, Wang Y. A segmentation method of smoke in forest-fire image based on fbm and region growing. 2011 Fourth International Workshop on Chaos-Fractals Theories and Applications. IEEE, 2011: 390-393.

[2] Xing D, Zhongming Y, Lin W, et al. Smoke image segmentation based on color model. Journal on Innovation and Sustainability RISUS, 2015, 6(2): 130-138.

Traditional Smoke Segmentation

Others focus on the clustering technique and morphology characteristics of smoke.

Iterative clustering, superpixel segmentation [3]

Morphology [4]

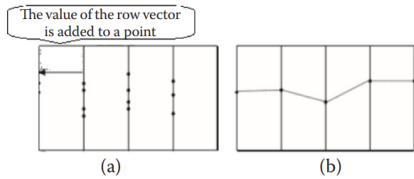
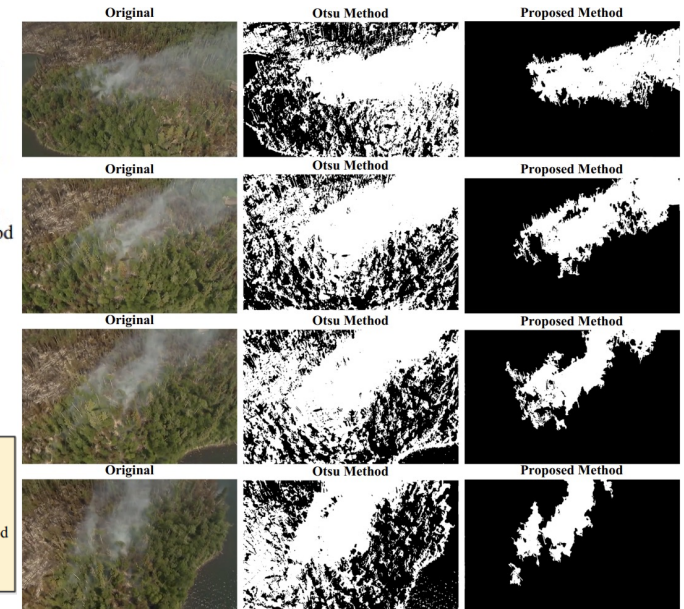
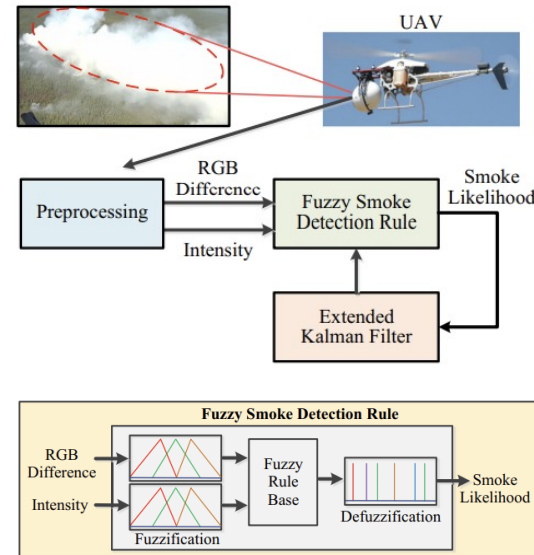
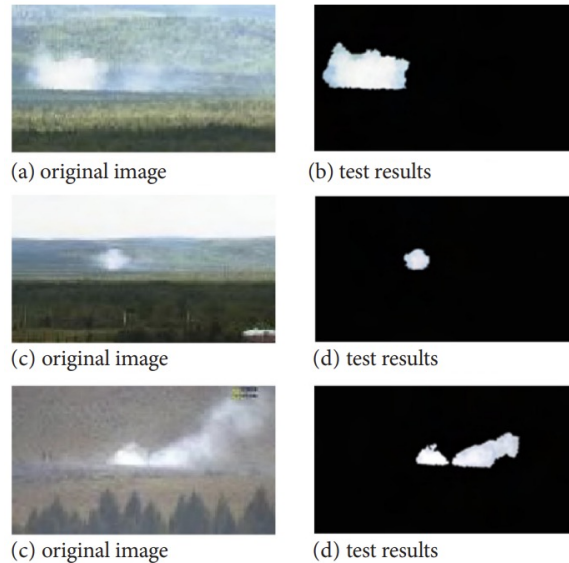
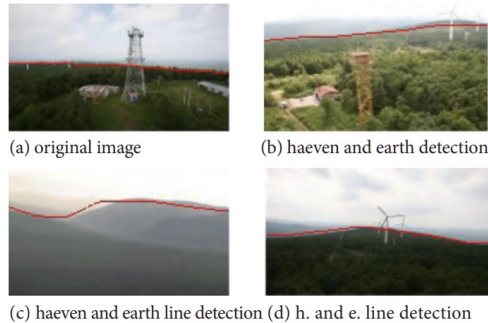


Fig. 1. Horizontal line detection: (a) candidate point selection, (b) division of the horizon



[3] Xiong D, Yan L. Early smoke detection of forest fires based on SVM image segmentation. Journal of Forest Science, 2019, 65(4): 150-159.

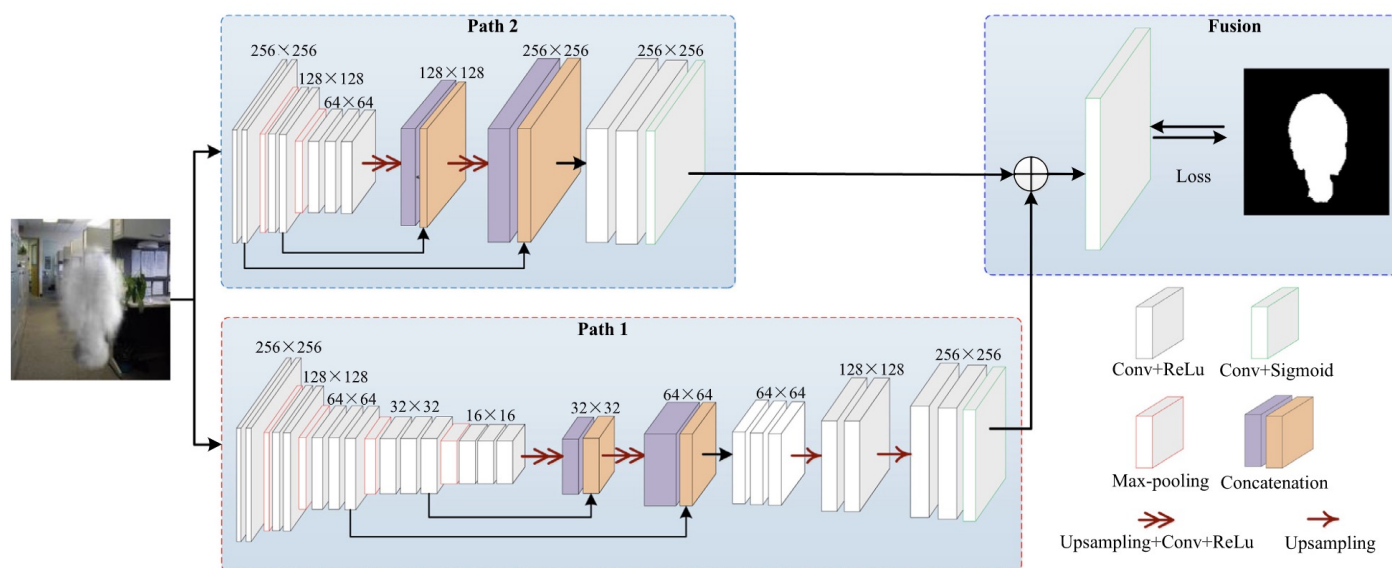
[4] Yuan C, Liu Z, Zhang Y. Learning-based smoke detection for unmanned aerial vehicles applied to forest fire surveillance. Journal of Intelligent & Robotic Systems, 2019, 93: 337-349.

Smoke segmentation based on deep learning

- Larger receptive fields to cope with the **variability** and **blurred edges** of smoke.

DSS [5]

- **Dual-channel encoder-decoder**
- One channel is used to coarsely extract **global** information
- The other channel is utilized to finely extract **local** information.



dual-channel encoder-decoder architecture

Smoke Image

(a)

FCN

(b)

SegNet

(c)

Deeplab v1

(f)

Yuan et al. [5]

(i)

Label Noise

Images labelled as cat



Images labelled as dog

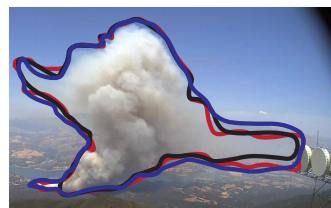


— mislabelled image
— correctly labelled image

- Noisy labels are almost inevitable in smoke segmentation.
- Smoke edges are complex and blurry, making it hard to distinguish smoke and background.
- Smoke is non-rigid and lacks a fixed shape, making it difficult for annotators to become proficient through practice with the same shape.



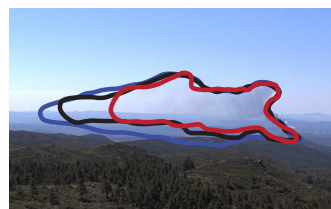
Regular Smoke



Regular Smoke Annotations



Early Smoke



Early Smoke Annotations

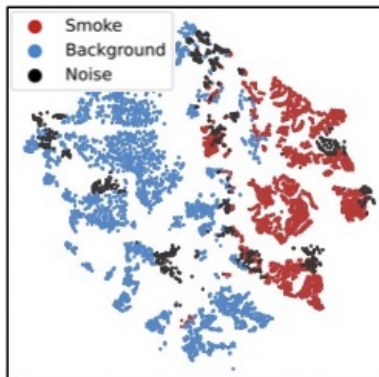
Motivation

*variable
transparency*



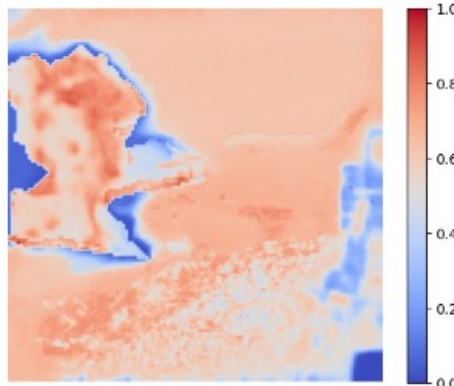
(a) Smoke Image

*inconsistent
features*



(b) Embeddings

- 1) How to determine the sample weight through prototypes.
- 2) How to update prototypes under noisy labels.



(c) CoSW

Total Entropy (based on Shannon entropy)

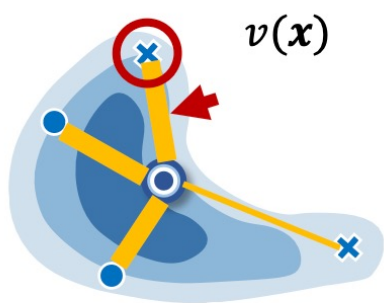
$$T = - \sum_{k=1}^{\Omega K} \sum_{n=1}^{N^k} \frac{v_n^k}{N} \ln \frac{v_n^k}{N},$$

Within-prototype Entropy (WE)

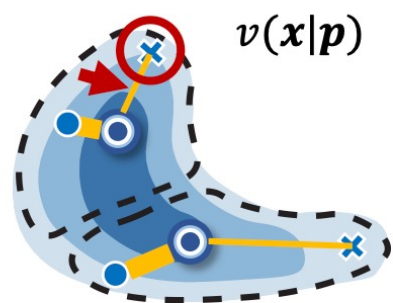
$$T_w = - \sum_{k=1}^{\Omega K} \frac{N^k}{N} \sum_{n=1}^{N^k} \frac{v_n^k}{N^k} \ln \left(\frac{v_n^k}{N^k} \right),$$

Between-prototype Entropy






$$T_b = - \sum_{k=1}^{\Omega K} \frac{N^k}{N} \ln \frac{N^k}{N},$$



Sample Weighting



Conditional Sample weighting

-  Prototype
-  Noisy Label
-  High Weight
-  Low Weight
-  Cluster

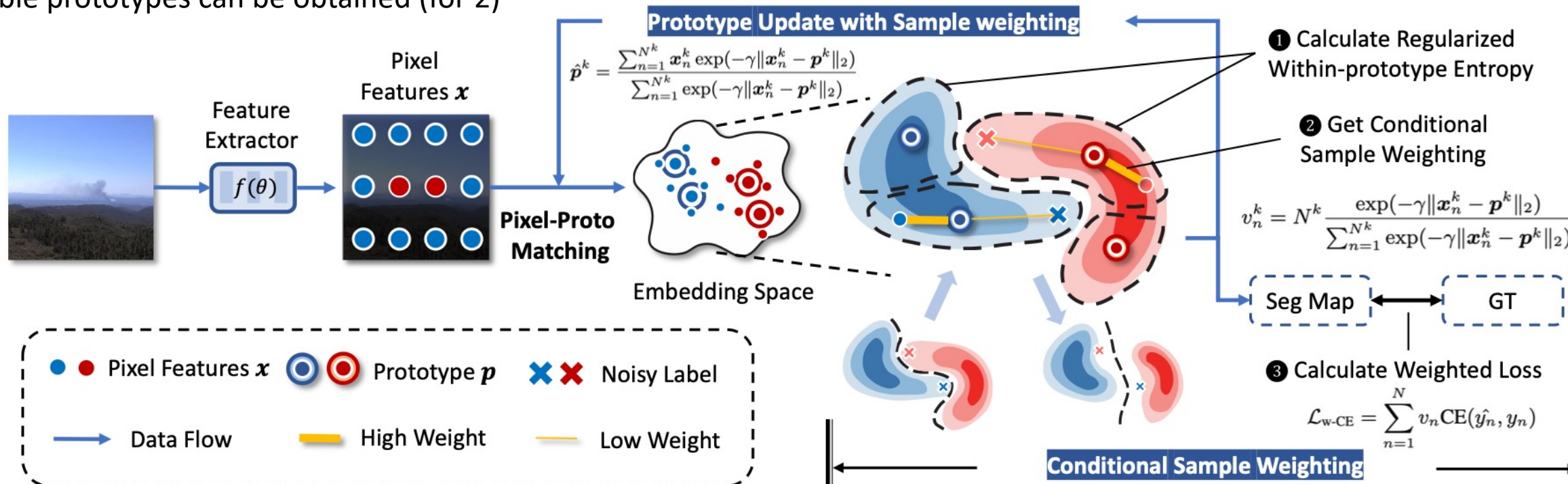
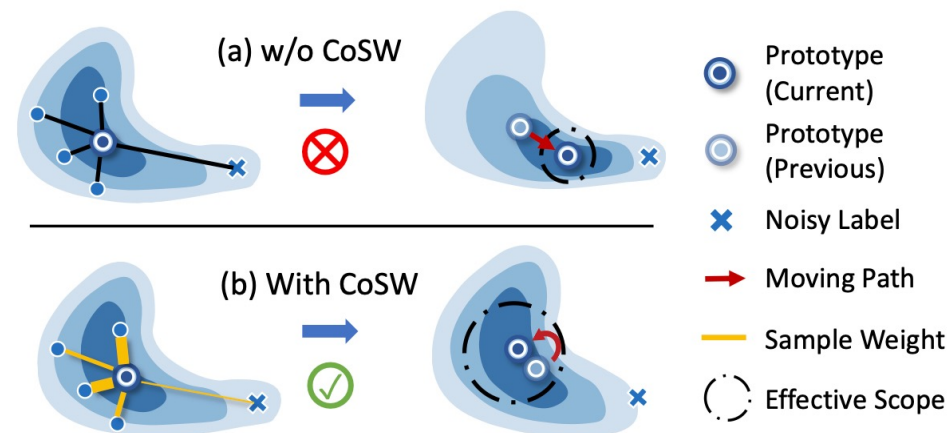
(d) Intuition of CoSW

CoSW Overview

Regularized Within-prototype Entropy (RWE)

$$J(P, V) = - \sum_{k=1}^{\Omega K} \frac{N^k}{N} \sum_{n=1}^{N^k} \frac{v_n^k}{N^k} \ln\left(\frac{v_n^k}{N^k}\right) - \gamma \sum_{k=1}^{\Omega K} \frac{N^k}{N} \sum_{n=1}^{N^k} \frac{v_n^k}{N^k} \|\mathbf{x}_n^k - \mathbf{p}^k\|_2,$$

- Consider the information between all pixels that matched the given prototype and obtain adaptive sample weights (for 1).
- Calculate the expectation of weighting samples, stable prototypes can be obtained (for 2)



Datasets

SmokeSeg (Real-world Noise)

- **Real-world** smoke segmentation dataset
- Most images are **early smoke**.



SMOKE5K (Real-world Noise)

- 4K synthetic images
- + 1K real-world images)



NS-1K (Synthetic Noise)



Smoke Image



Clean



Eroded



Dilated

Edge-distorted



Smoke Image



Clean



Eroded



Dilated

Edge-distorted

Comparison with State-of-the-Art Methods

	Methods	Backbone	Total		Small		Medium		Large	
			F_1	$mIoU$	F_1	$mIoU$	F_1	$mIoU$	F_1	$mIoU$
<i>Real-time</i>	AFFormer ^o [8]	AFFormer-B	58.41	47.89	45.98	34.10	64.52	53.20	66.96	54.15
	SeaFormer ^o [40]	SeaFormer-B	57.58	44.70	41.33	30.35	66.02	53.10	67.16	53.21
	SegFormer ^o [47]	MiT-B0	60.90	<u>48.53</u>	<u>48.31</u>	<u>35.69</u>	68.86	53.34	68.53	55.80
	SC [§] [52]	MiT-B0	59.78	47.70	45.76	33.15	68.37	55.68	66.13	53.96
	CleanNet* [27]	MiT-B0	<u>61.63</u>	47.00	47.16	33.57	66.23	50.91	70.96	56.22
	Ours	MiT-B0	62.98	48.62	49.85	36.64	<u>68.81</u>	<u>53.87</u>	<u>70.79</u>	<u>55.85</u>
<i>Normal</i>	DeeplabV3+ ^o [5]	ResNet-50	65.92	53.50	54.03	41.07	71.82	58.73	71.87	58.95
	OCRNet ^o [57]	HRNet-48	64.93	52.45	52.04	39.47	71.04	57.47	70.51	58.19
	SegNeXt ^o [13]	MSCAN-L	66.71	52.37	58.05	44.16	70.41	55.77	72.97	58.42
	Trans-BVM [†] [51]	ResNet-50	67.15	53.11	59.02	44.62	71.50	56.99	73.36	58.97
	Ours	ResNet-50	68.49	54.09	61.27	46.28	72.31	58.08	<u>74.78</u>	60.81
	SegFormer ^o [47]	MiT-B3	67.70	53.37	57.67	45.21	<u>73.87</u>	<u>60.49</u>	72.06	58.52
	Trans-BVM [†] [51]	MiT-B3	67.68	53.09	60.85	45.87	71.73	57.35	73.51	59.10
	SC [§] [52]	MiT-B3	69.55	55.04	<u>62.26</u>	<u>48.47</u>	71.41	57.06	72.91	58.23
	CleanNet* [27]	MiT-B3	<u>70.17</u>	<u>56.94</u>	61.98	48.05	73.06	59.07	74.57	<u>60.93</u>
	Ours	MiT-B3	72.32	59.25	64.62	50.86	74.37	61.14	75.52	62.30

Comparison with State-of-the-Art Methods

(a) Comparison on SMOKE5K.

Methods	F_β	$mIoU$
OCRNet ^o [57]	72.51	63.00
DeeplabV3+ ^o [5]	73.83	64.08
SegNeXt ^o [13]	76.44	67.08
Trans-BVM [†] [51]	76.23	67.55
Ours	77.02	67.58
SegFormer ^o [47]	78.68	68.29
Trans-BVM [†] [51]	78.91	68.97
SC [§] [52]	79.33	69.40
CleanNet* [27]	80.37	70.23
Ours	81.71	71.24

(b) Comparison on the synthetic noisy dataset NS-1K.

		Trans-BVM [†] [51]		SC [§] [52]		CleanNet* [27]		Ours	
Noise Ratio	Noise Intensity	F_1	$mIoU$	F_1	$mIoU$	F_1	$mIoU$	F_1	$mIoU$
0%	-	52.79	39.12	51.94	37.84	52.02	38.24	<u>52.59</u>	<u>38.32</u>
20%	Low	51.91	38.16	<u>51.81</u>	<u>37.94</u>	51.21	37.24	51.77	37.58
	High	48.02	34.52	51.14	37.15	50.34	36.31	<u>50.99</u>	<u>36.80</u>
40%	Low	45.40	32.30	<u>49.69</u>	<u>35.89</u>	49.09	35.53	50.18	36.69
	High	41.09	28.15	45.31	32.16	<u>46.08</u>	<u>33.15</u>	48.34	34.73
60%	Low	42.73	29.01	44.12	30.87	<u>46.33</u>	<u>33.96</u>	48.38	35.34
	High	40.57	27.50	41.77	28.44	<u>43.69</u>	<u>29.87</u>	45.86	32.08
80%	Low	39.28	26.42	40.52	27.42	<u>42.96</u>	<u>29.37</u>	44.40	31.24
	High	37.38	25.58	39.09	25.88	<u>40.27</u>	<u>27.21</u>	42.37	29.89

Ablation Study

(a) Ablation study of CoSW (dataset: SmokeSeg).

	Proto	Sample Weight	Proto Weight	F_1	$mIoU$
bl				67.70	53.37
(1)	✓			68.17 ↑ 0.47	55.23 ↑ 1.86
(2)	✓	✓		70.04 ↑ 2.34	56.40 ↑ 3.03
(3)	✓		✓	69.38 ↑ 1.68	55.72 ↑ 2.35
(4)	✓	✓	✓	71.39 ↑ 3.69	57.68 ↑ 4.31

Table 4: Different entropies.

	F_1	$mIoU$
Kapur's Entropy	71.34	58.38
Burg's Entropy	69.20	55.72
Shannon's Entropy	72.32	59.25

- Burg's Entropy

$$T^B(\Pi) = - \sum_{i=1}^N \ln \pi_i.$$

$$\max_{P,V} J^B(P,V) = - \sum_{k=1}^{\Omega K} \sum_{n=1}^{N^k} \ln \left(\frac{v_n^k}{N^k} \right)$$

$$- \gamma \sum_{k=1}^{\Omega K} \frac{N^k}{N} \sum_{n=1}^{N^k} \frac{v_n^k}{N^k} \|\mathbf{x}_n^k - \mathbf{p}^k\|_2.$$

$$v_n^k = N^k \frac{(-\gamma \|\mathbf{x}_n^k - \mathbf{p}^k\|_2)}{\sum_{n=1}^{N^k} (-\gamma \|\mathbf{x}_n^k - \mathbf{p}^k\|_2)},$$

$$\hat{\mathbf{p}}^k = \frac{\sum_{n=1}^{N^k} \mathbf{x}_n^k (-\gamma \|\mathbf{x}_n^k - \mathbf{p}^k\|_2)}{\sum_{n=1}^{N^k} (-\gamma \|\mathbf{x}_n^k - \mathbf{p}^k\|_2)},$$

- Kapur's Entropy

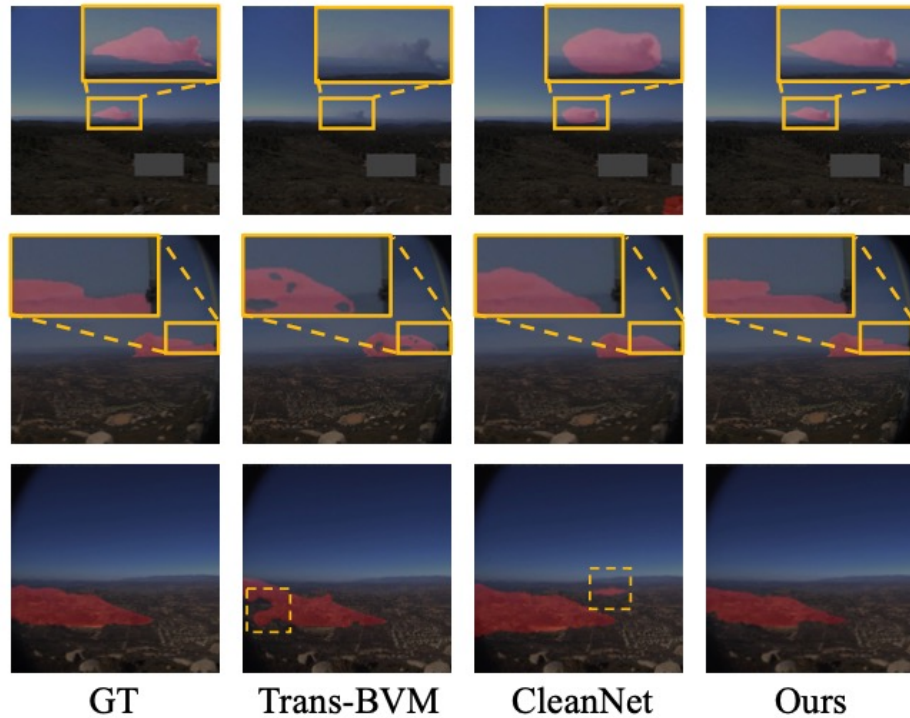
$$T^K(\Pi) = - \sum_{i=1}^N \pi_i \ln \pi_i - \sum_{i=1}^N (1 - \pi_i) \ln(1 - \pi_i).$$

$$\begin{aligned} \max_{P,V} J^K(P,V) = & - \sum_{k=1}^{\Omega K} \frac{N^k}{N} \sum_{n=1}^{N^k} \frac{v_n^k}{N^k} \ln \left(\frac{v_n^k}{N^k} \right) \\ & - \sum_{k=1}^{\Omega K} \frac{N^k}{N} \sum_{n=1}^{N^k} \left(1 - \frac{v_n^k}{N^k} \right) \ln \left(1 - \frac{v_n^k}{N^k} \right) \\ & - \gamma \sum_{k=1}^{\Omega K} \frac{N^k}{N} \sum_{n=1}^{N^k} \frac{v_n^k}{N^k} \|\mathbf{x}_n^k - \mathbf{p}^k\|_2. \end{aligned}$$

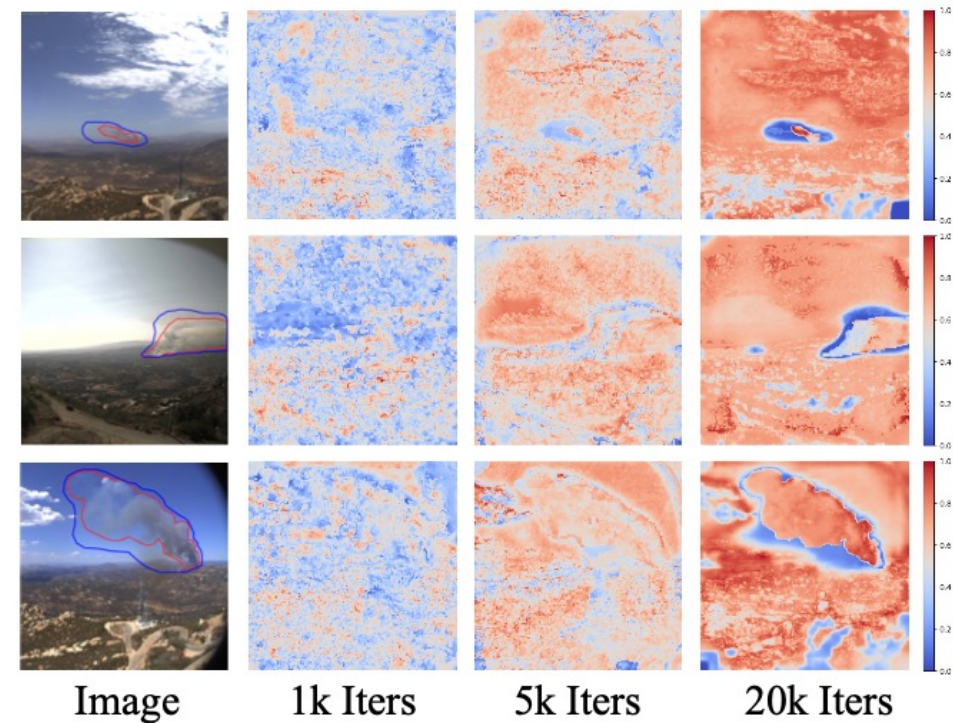
$$v_n^k = N^k \frac{1}{1 + \exp(-\|\mathbf{x}_n^k - \mathbf{p}^k\|_2 - \lambda_k)^\gamma},$$

$$\hat{\mathbf{p}}^k = \sum_{n=1}^{N^k} \frac{\mathbf{x}_n^k}{1 + \exp(-\|\mathbf{x}_n^k - \mathbf{p}^k\|_2 - \lambda_k)^\gamma},$$

Visualization



(a) Comparison of segmentation results in different scales.



(b) The formation process of CoSW (blue curve for noisy labels, and red for clean in the first image column).

To determine whether the prototype is clean, it is necessary to introduce clean validation, which is not implemented in our work. This is also a direction for further research.



華東理工大學

EAST CHINA UNIVERSITY OF SCIENCE AND TECHNOLOGY



THANK YOU

Lujian Yao